

## CHAPTER 219

### THE TIME DOMAIN ANALYSIS ON MOORED SHIP MOTIONS

Masayoshi KUBO\*  
M.JSCE, Dr.Eng., Associate Professor

Naokatsu SHIMODA\*\*  
M.JSCE, B.Eng., Vice-Head

Shunsaku OKAMOTO\*\*\*  
B.Sc.

#### ABSTRACT

The ship refuge inside a harbor in storm requires the analysis of moored ship motions along a quay wall. In this case the time domain analysis with the convolution integral method becomes effective. But the calculation accuracy is not enough and must be improved to analyze actual moored ship motions. In this paper some methods of the improvement are proposed and their efficiency is verified by comparing the calculation results with the experimental ones.

#### 1. INTRODUCTION

Recently, many developments in the coastal zone are planned in Japan, for example the construction of artificial islands and so on. Since the reclamations of the sea narrow the anchoring areas outside a harbor in storm, the ship refuge inside a harbor in storm has been investigated by the Ministry of Transport.

When moored ship motions along a quay wall are considered, the time domain analysis with the convolution integral method becomes effective. But the papers with this method are very few<sup>1)2)</sup> and moreover the calculation accuracy for actual moored ship motions does not seem to be satisfactory. In this paper, some calculation methods are proposed to improve the accuracy and their efficiency is verified by comparing the calculation results with the experimental ones.

---

\* Associate Professor, Kobe University of Mercantile Marine  
1-1, 5-Chome, Fukae-Minami-Machi, Higashinada-Ku, Kobe  
658, Japan

\*\* Vice-Head, Technical Laboratory, Giken Kogyo Co., LTD.  
1540, Kawaguchi-Cho, Hachiohji 193, Japan

\*\*\* Technical Laboratory, Giken Kogyo Co., LTD.  
1540, Kawaguchi-Cho, Hachiohji 193, Japan

## 2. ON HYDRODYNAMIC COEFFICIENTS

## 2.1 Calculation Method

## a) Equations of Ship Motions in the Time Domain

The calculations and the experiments are carried out by using the model ship shown in Fig.-1. The model is a rectangular floating body moored symmetrically along a quay wall. The incident wave angle  $\theta$  is 60 (deg). The equation of ship motions in the time domain and the coefficients are given by,

$$\begin{aligned} \sum_{i=1}^6 \{M_{ij} + m_{ij}(\infty)\} \ddot{x}_i(t) \\ + \sum_{i=1}^6 \int_{-\infty}^t \dot{x}_i(\tau) L_{ij}(t-\tau) d\tau \\ + \sum_{i=1}^6 (C_{ij} + G_{ij}) x_i(t) = F_j, \quad (1) \end{aligned}$$

(j=1, 2, ..., 6)

$$L_{ij}(t) = \frac{2}{\pi} \int_0^{\infty} B_{ij}(\omega) \cos \omega t d\omega, \quad (2)$$

$$\begin{aligned} m_{ij}(\infty) = A_{ij}(\omega) \\ + \frac{1}{\omega} \int_0^{\infty} L_{ij}(t) \sin \omega t dt, \quad (3) \end{aligned}$$

where  $x_i(t)$ =displacement,  $M_{ij}$ =mass or moment of inertia,  $m_{ij}(\infty)$ =constant added mass or constant added moment of inertia,  $L_{ij}(t)$ =retardation function,  $C_{ij}$ =hydrostatic restoring force coefficient,  $G_{ij}$ =mooring force coefficient,  $F_j$ =external force,  $t$ =time,  $\tau$ =integral variable,  $A_{ij}(\omega)$ =added mass or added moment of inertia (which is called added mass hereafter) and  $B_{ij}(\omega)$ =damping coefficient which correspond to the angular frequency  $\omega$ . The subscripts  $i$  and  $j$  describe the mode of ship motions, namely, 1:Sway, 2:Surge, 3:Heave, 4:Pitch, 5:Roll and 6:Yaw. The coefficients with the subscript  $ij$  show the effect on the  $i$ -th mode from the motion of the  $j$ -th mode.

As is obvious from the above, the hydrodynamic coefficients in Eq.(1) are decided by calculating the

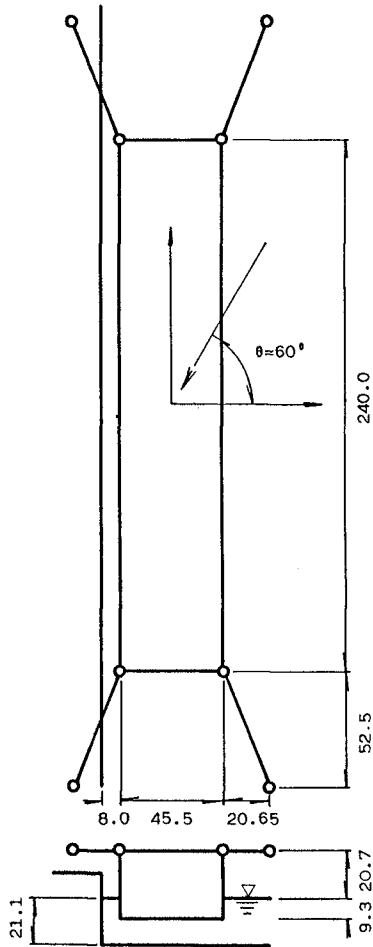


Fig.-1 The model ship  
(unit:cm)

frequency dependent added mass and the damping coefficient.

b) Calculation of Added Mass and Damping Coefficient

The added mass and the damping coefficient are calculated by the method of Green's function. Then the length of the mesh must be divided into less than a quarter of the wave length, so that the meshes represent the wave profile. In the case shown in Fig.-1, there are 18 coupling terms of  $A_{ij}(\omega)$  and  $B_{ij}(\omega)$  as shown in Table-1 because of the influence of the reflected waves. Further, the number of coupling terms is decreased to 12 by confirming the symmetry of the hydrodynamic coefficients,  $A_{ij}(\omega)=A_{ji}(\omega)$  and  $B_{ij}(\omega)=B_{ji}(\omega)$ .

c) Calculation of Retardation Function

Since the damping coefficients in the whole angular frequency are required to calculate the retardation functions by Eq.(2), the damping coefficients must be approximated in the higher frequency than the maximum calculation angular frequency. In the two dimensional case the approximating formula for the higher frequency is given by Takagi and Saito<sup>3)</sup> as follows,

$$B_{ij}(\omega)=k_{ij} \omega^{-n}, \quad (4)$$

where  $k_{ij}$  is a coefficient for joining calculated values to approximated ones and  $n$  is a multiplier. It's considered that the same approximation can be possible in the three dimensional case, then the values of  $n$  are given as shown in Table-2.

As mentioned above, the retardation functions are given by substituting Eq.(4) into Eq.(2).

Table-1 The coupling between each motion mode

		i					
		1	2	3	4	5	6
j		Sway	Surge	Heave	Pitch	Roll	Yaw
1	Sway	o	x	o	x	o	x
2	Surge	x	o	x	o	x	o
3	Heave	o	x	o	x	o	x
4	Pitch	x	o	x	o	x	o
5	Roll	o	x	o	x	o	x
6	Yaw	x	o	x	o	x	o

o = coupling term

x = no coupling term

Table-2 The values of n in Eq.(4)

i \ j		1	2	3	4	5	6
		Sway	Surge	Heave	Pitch	Roll	Yaw
1	Sway	3	-	5	-	5	-
2	Surge	-	3	-	5	-	3
3	Heave	5	-	7	-	7	-
4	Pitch	-	5	-	7	-	5
5	Roll	5	-	7	-	7	-
6	Yaw	-	3	-	5	-	3

$$L_{ij}(t) = \frac{2}{\pi} \left\{ \int_0^{\omega_e} B_{ij}(\omega) \cos \omega t d\omega + k_{ij} \int_{\omega_e}^{\infty} \omega^{-n} \cos \omega t d\omega \right\}, \tag{5}$$

where  $\omega_e$  is the maximum calculation angular frequency. The analytical integral in the second term of the right hand side can be carried out by using the integration by parts and cosine integral.

d) Calculation of Constant Added Mass

The retardation functions are also required in the whole time domain to calculate the constant added masses in Eq.(3). On the other hand, the retardation functions show the decreasing oscillatory curve, so they are approximated by the next Eq.,

$$L_{ij}(t) = r e^{-pt} \cos(qt + \epsilon), \tag{6}$$

where  $r, p, q$  and  $\epsilon$  are arbitrary constants. And the damping coefficients are given by applying the inversion formula of Fourier transform to Eq.(2),

$$B_{ij}(\omega) = \int_0^{\infty} L_{ij}(t) \cos \omega t dt. \tag{7}$$

Substituting Eq.(6) into Eq.(7) and carrying out the integrations by parts in the right hand side, then Eq.(8) is obtained,

$$B_{ij}(\omega) = \frac{r}{2} \left\{ \frac{p \cos \epsilon - (q + \omega) \sin \epsilon}{p^2 + (q + \omega)^2} + \frac{p \cos \epsilon - (q - \omega) \sin \epsilon}{p^2 + (q - \omega)^2} \right\}, \tag{8}$$

where the constants  $r, p, q$  and  $\epsilon$  are decided by comparing the values obtained from Eq.(6) and (8) with ones from the numerical integral calculation. The truncation error  $S_p$  which is occurred from the halfway end of the infinite integral Eq.(7) is defined by using these constants and the

end time of the integral  $t_e$ , namely,

$$Sp = \frac{\int_0^{t_e} e^{-pt} \cos(qt + \epsilon) \sin \omega t dt}{A_{ij}(\omega) + \frac{1}{\omega} \int_0^{t_e} L_{ij}(t) \sin \omega t dt} \quad (9)$$

Since both the numerator and the denominator in Eq.(9) can be calculated analytically,  $t_e$  for the enough accuracy can be decided by Eq.(9). Eventually, the infinite integral in Eq.(3) is changed to the finite integral from 0 to  $t_e$ .

### 2.3 Calculation Results

#### a) Added Mass and Damping Coefficient

The length of the mesh is decided as the value which makes the maximum calculation angular frequency  $\omega_e$  10.0 ( $2\pi/\text{sec}$ ). To confirm the symmetry of the hydrodynamic coefficients, the added masses and the damping coefficients in the case of  $i=1, j=5$  and  $i=5, j=1$  are shown in Fig.-2. In the figure the dotted line shows the case of  $i=1, j=5$ , the broken line shows the case of  $i=5, j=1$  and the solid line shows the average values of them. Good agreements between the results of the two cases are obtained but there are a little difference. So the average values are used in the cases of  $i \neq j$  hereafter.

In Fig.-2, there is a discontinuous value at  $\omega=7.9$  ( $2\pi/\text{sec}$ ). In particular, the value of the damping coefficient is negative at this frequency, therefore, the calculation of ship motions diverges. So we use the smoothed value at the angular frequency as shown in Fig.-3.

#### b) Retardation Function

The damping coefficients are shown in Fig.-4. The solid line shows the calculation results and the dotted line shows the approximate curve by Eq.(4). The results in the range from 10.0 to 14.0 ( $2\pi/\text{sec}$ ) become valid by shortening the mesh length to a half and the converging tendency proves the validity of the approximation. The converging tendency of all damping coefficients in the high angular frequency is completed by the results of B22.

The retardation functions by Eq.(5) are shown in Fig.-5. The abscissas show the elapsed time.

#### c) Constant Added Mass

As an example, the value of  $t_e$  will be shown in the case of  $i=5, j=5$ . The approximate results of the retardation functions and the damping coefficients by Eq.(6) and (8) are shown as the solid line in Fig.-6. The dotted line shows the damping coefficients by the numerical calculation, when  $r=1.6 \times 10^8$  ( $g \cdot \text{cm}^2/\text{sec}^2$ ),  $p=0.416$  ( $1/\text{sec}$ ),  $q=5.153$  ( $1/\text{sec}$ ) and  $\epsilon=0$ . The relation between  $t_e$  and  $Sp$  is shown in Fig.-7. Since  $Sp$  is less than 0.01 at  $t_e=20$  (sec),  $t_e$  is decided 60 (sec) to secure the calculation accuracy.

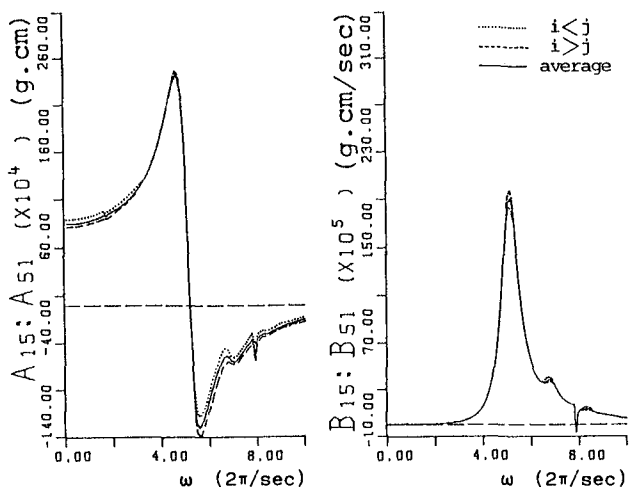


Fig.-2 The added mass and the damping coefficient

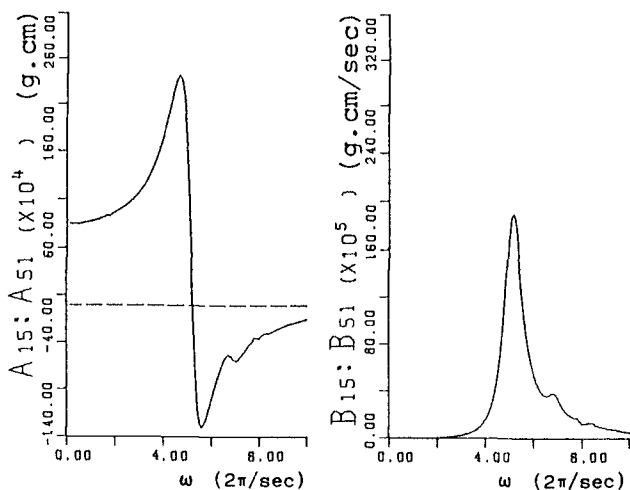


Fig.-3 The smoothed added mass and the damping coefficient

Next, the constant added masses calculated by using the  $t_e$  and Eq.(3) are shown as the thick lines in Fig.-8. The thin lines show the average values of them and the two-dot-dash-lines show the added masses which correspond to the angular frequency  $\omega$ . It can be considered that the constant added masses show the constancy on the angular frequency.

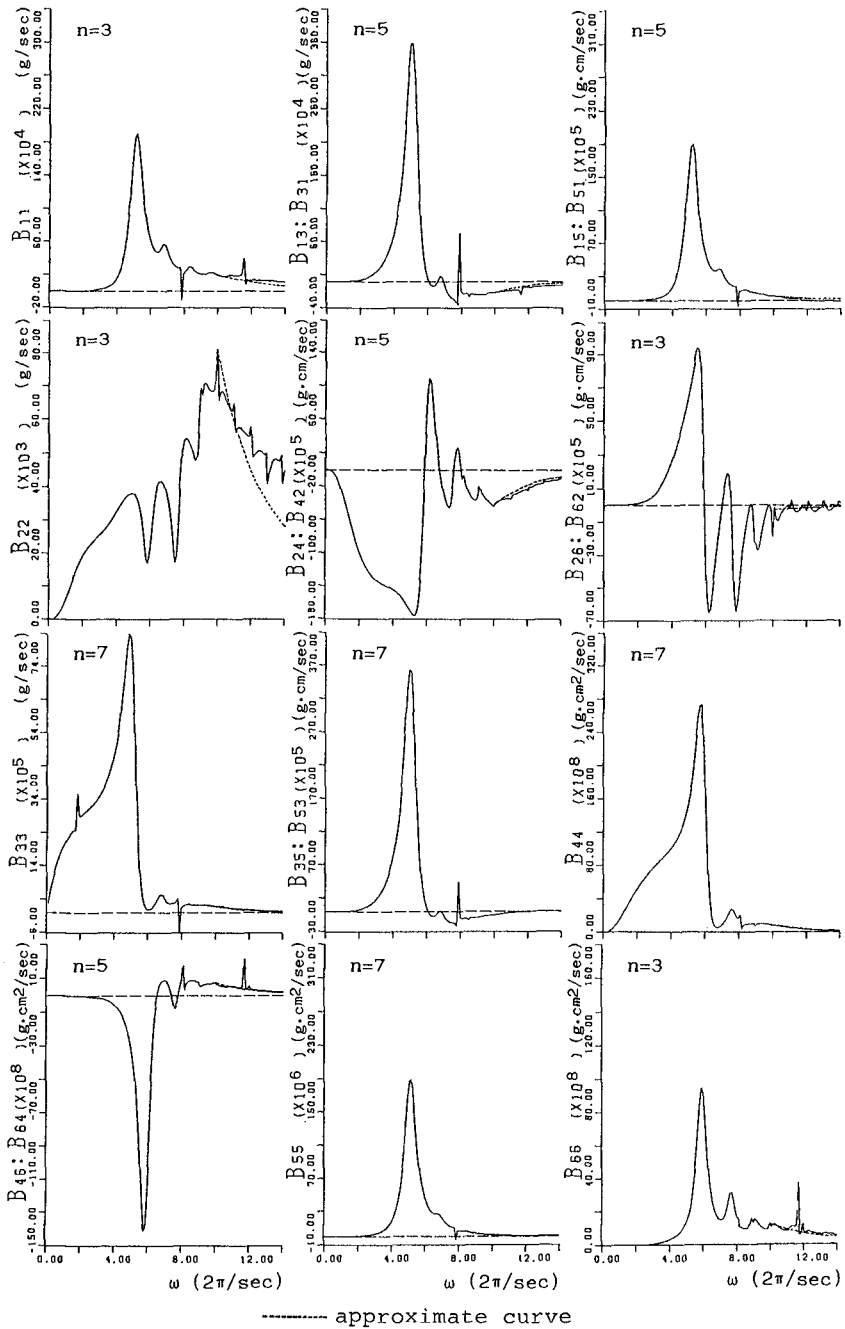


Fig.-4 The approximate curves of the damping coefficients

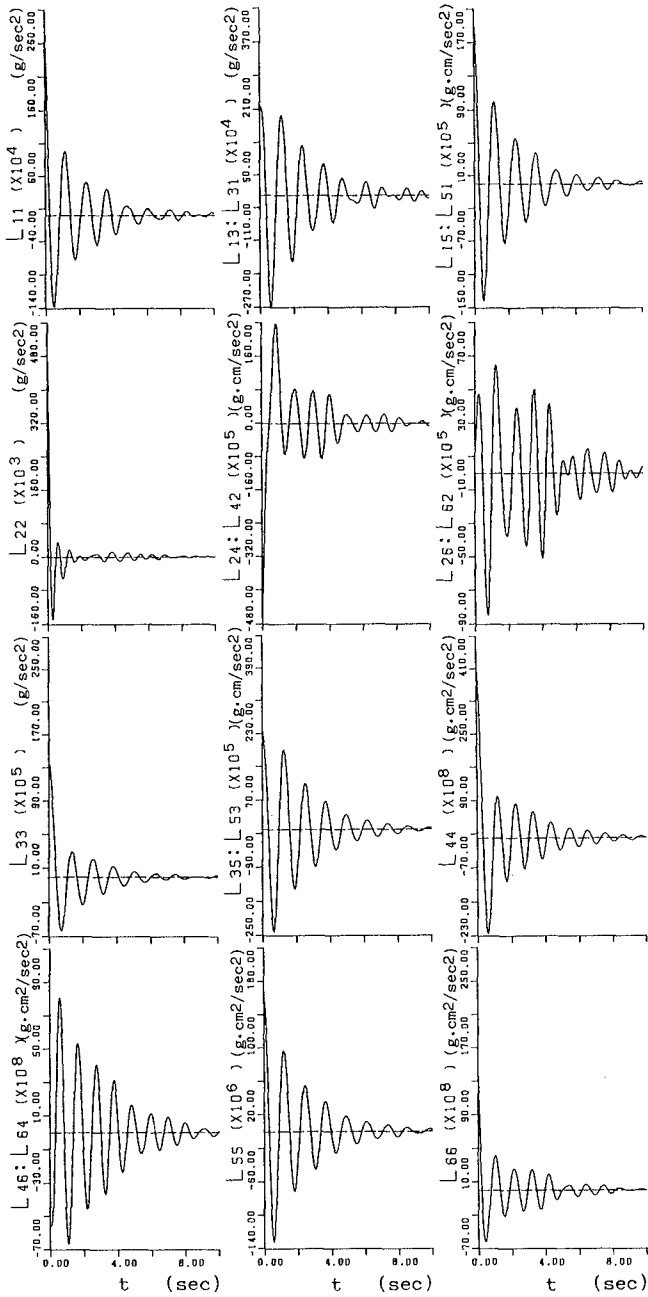


Fig.-5 The retardation functions

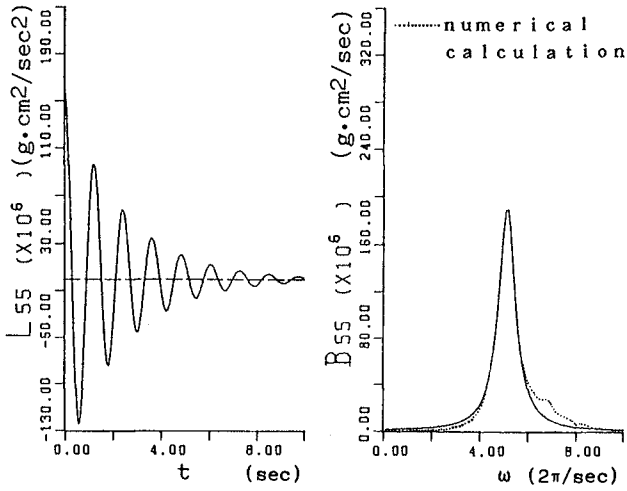


Fig.-6 The approximate results of the retardation function and the damping coefficient

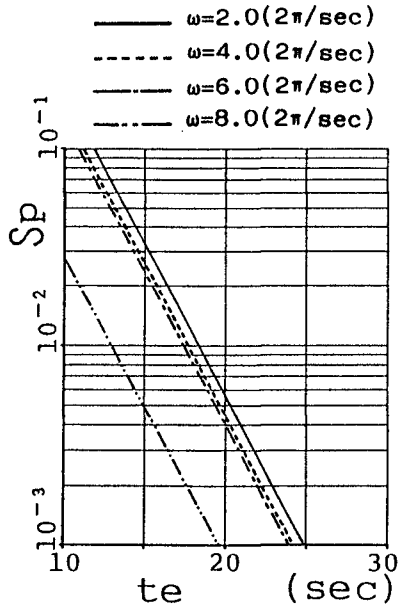


Fig.-7 The relation between  $t_e$  and  $Sp$

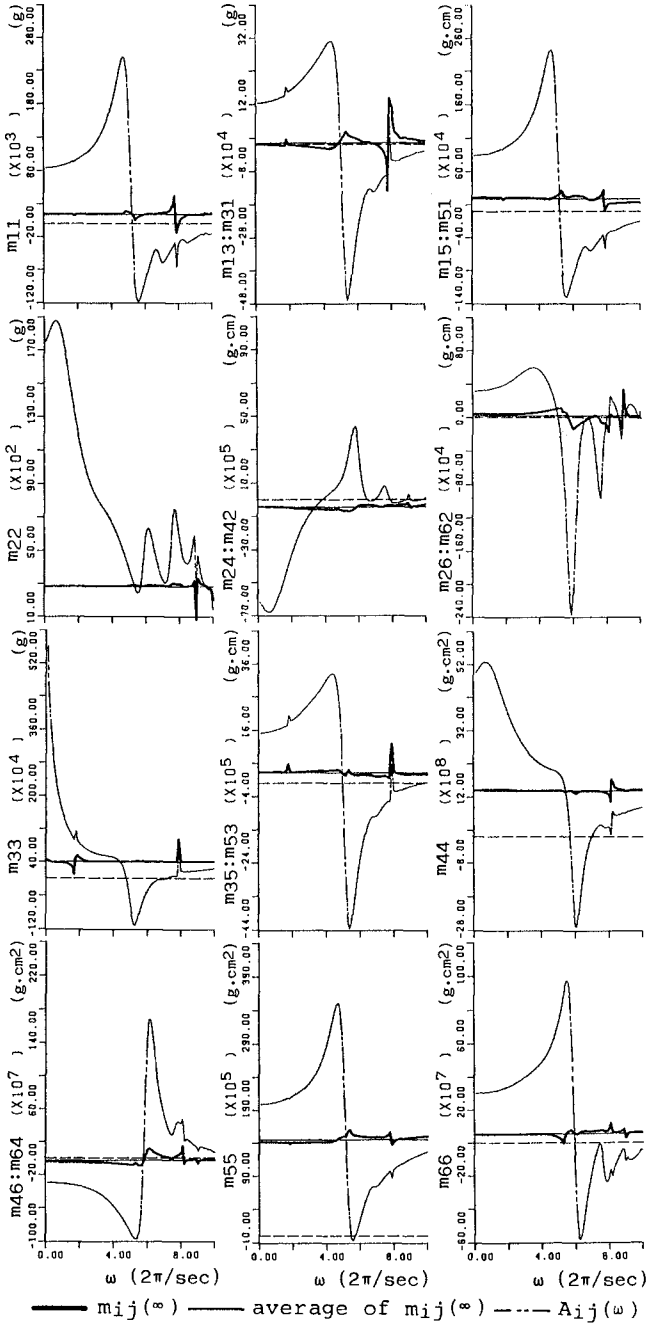


Fig.-8 The constant added masses

### 3. TIME DOMAIN ANALYSIS

#### 3.1 Calculation Method

A time domain analysis can be carried out by calculating Eq.(1) with the obtained results. But the attention should be paid to the following matters.

##### a) Natural Period

Since the potential theory dose not give the viscosity term, the amplitude of ship motions is overestimated at the natural period because of the lack of damping force. Therefore, the existence of the natural period must be investigated within the range of used period. The natural period is obtained from the calculation of the free oscillations by giving an initial displacement in Eq.(1).

##### b) Introduction of Viscosity Term

The calculations are corrected by introducing the viscosity term  $N_i \cdot x_i(t)$  to the second term of the left hand side in Eq.(1). The coefficient  $N_i$  is decided so that the calculated amplification factors of ship motions coincide with the experimental ones at the natural periods.

#### 3.2 Calculation Results

##### a) Natural Period

The calculation results of the free oscillations are shown in Fig.-9. Each natural period is 10.1 (sec) in Sway, 3.8 (sec) in Surge, 0.8 (sec) in Heave, 0.8 (sec) in Pitch, 1.4 (sec) in Roll and 9.6 (sec) in Yaw.

##### b) Ship Motions in Beam Seas

The calculations are carried out in the range of the incident wave period from 0.6 to 2.4 (sec) and the results are compared with the experimental ones. The viscosity terms are introduced in Heave and Roll which have the natural periods in the above wave period range. The viscosity damping are evaluated by the logarithmic damping coefficient  $\lambda$ . The calculated free oscillations and the experimental ones are shown in Fig.-10. The ordinates,  $\alpha$ , show the ratio of the displacement to the initial one.  $\lambda$  of Heave is varied widely because of the considerable change of the neighboring wave amplitude ratio. In Roll, 0.58 of  $\lambda$  is suitable for the calculations of ship motions, but 0.26 of  $\lambda$  is adequate for the above free oscillations. That is to say, the viscosity coefficient in ship motions is bigger than the one in the free oscillations. The difference may be modified by considering that the viscosity force is in proportional to the velocity squared.

Both results of the experiments and the calculations with and without the viscosity terms are shown in Fig.-11.

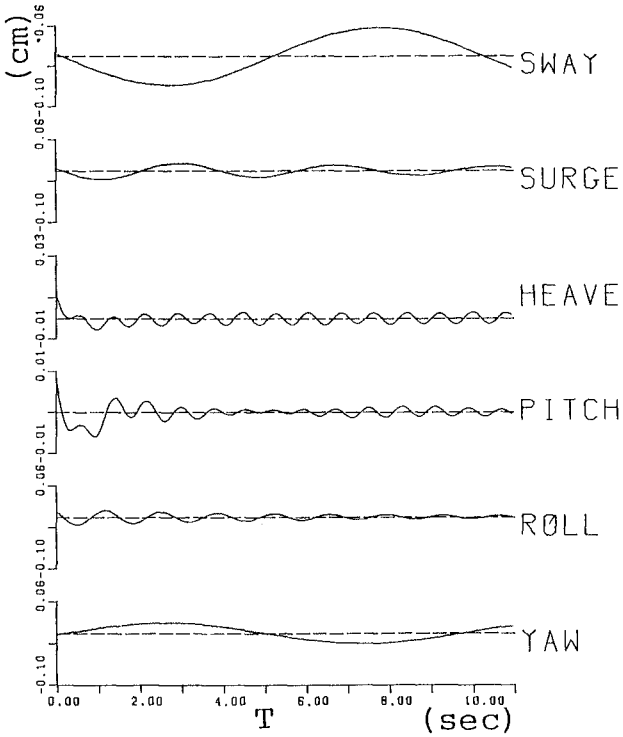


Fig.-9 The free oscillations

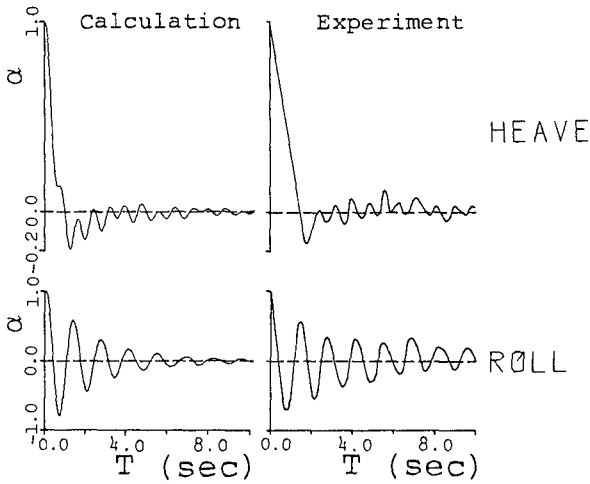


Fig.-10 The experiments and the calculated free oscillations with the viscosity terms

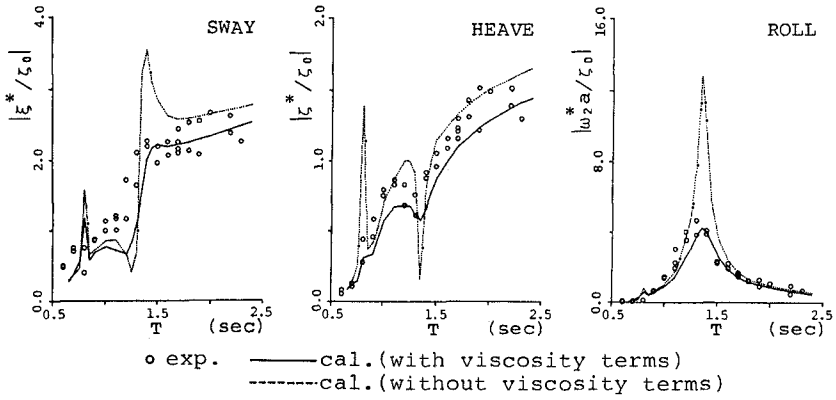


Fig.-11 The calculations and the experiments in the beam sea

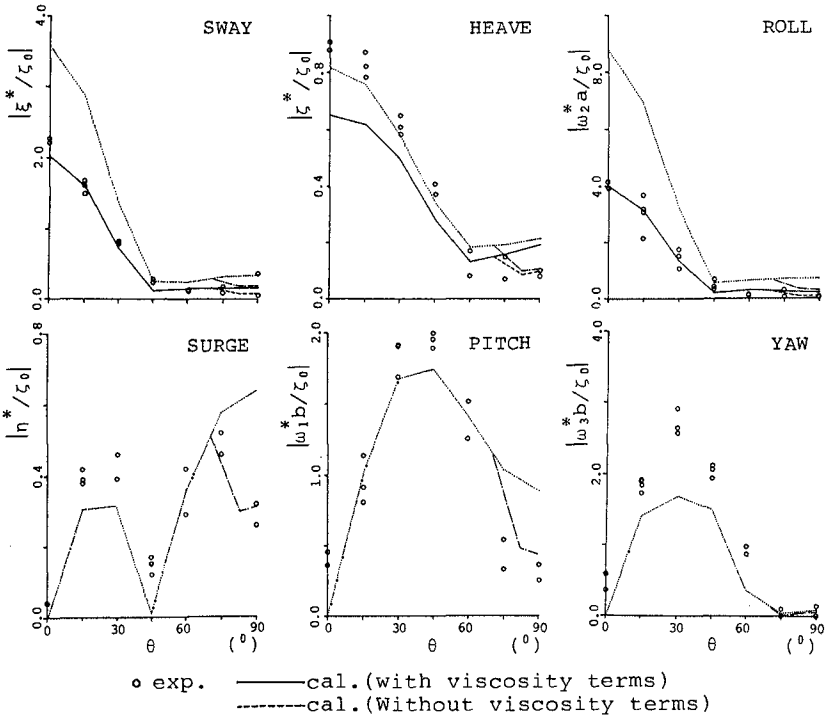


Fig.-12 The calculations and the experiments when the incident wave period is fixed at 1.4 (sec) and the incident wave angle is changed.

The ordinates show the amplification factor of ship motions.  $\xi^*$ ,  $\zeta^*$  and  $\omega_2^*$  correspond to the complex amplitudes of Sway, Heave and Roll.  $\zeta_0$  is the incident wave amplitude and  $a$  is a half ship width. On Sway and Roll, the correction by the viscosity term is effective, but on Heave the correction tends to be overestimated except in the vicinity of the natural period.

#### c) Ship Motions in Oblique Waves

When the incident wave period is fixed at 1.4 (sec) and the incident wave angle  $\theta$  is changed, the results are shown in Fig.-12. The ordinates show the amplification factor of ship motions. The abscissas  $\theta$  show the incident wave angle and  $\theta=0$  (deg) corresponds to the beam sea.  $\eta^*$ ,  $\omega_1^*$  and  $\omega_3^*$  correspond to the complex amplitudes of Surge, Pitch and Yaw.  $b$  is a half ship length and the others are the same in Fig.-11. The viscosity terms are not introduced into Surge, Pitch and Yaw because of the disagreement between the wave period and the natural periods. The dotted line and the one-dot-dash-line show the results corrected by considering the effect of the finite length of a quay wall when  $\theta$  is bigger than 75 (deg). It can be seen from Fig.-12 that there is a little error in the modes except Sway and Roll.

#### 4. CONCLUSION

It is confirmed that the calculation accuracy is advanced by the improvement of the calculation methods on the retardation functions, the constant added masses and the introduction of the viscosity terms into equation of ship motions. But the introduction of the viscosity terms into the other modes where the viscosity forces are not considered in this paper must be discussed hereafter. They will be a main problem when the long period ship motions are calculated.

#### REFERENCES

- 1) Swaragi, T., M. Kubo and S. Aoki: New mooring system to reduce ship motions and berthing energy, Coastal Engineering in Japan, pp.303-313, Vol.27, 1984.
- 2) Oortmerssen, G. Van: The motions of a moored ship in waves, Publication No.510, Netherlands Ship Model Basin, Wageningen, The Netherlands, 1976.
- 3) Takagi, M. and K. Saito: On the description of non-harmonic wave problems in the frequency domain (5-th report), Journal of the Kansai Society of Naval Architects, Japan, pp.51-59, No.191, 1983 (in Japanese).